

Antiferromagnetism in Ru_2MnZ ($Z = \text{Sn, Sb, Ge, Si}$) full Heusler alloys: Effects of magnetic frustration and chemical disorder

Sergii Khmelevskiy,¹ Eszter Simon,¹ and László Szunyogh^{1,2}

¹*Department of Theoretical Physics, Budapest University of Technology and Economics, Budafoki út 8., H-1111 Budapest, Hungary*

²*MTA-BME Condensed Matter Research Group, Budapest University of Technology and Economics, Budafoki út 8., H-1111 Budapest, Hungary*

(Received 17 January 2015; revised manuscript received 13 March 2015; published 30 March 2015)

We present systematic theoretical investigations to explore the microscopic mechanisms leading to the formation of antiferromagnetism in Ru_2MnZ ($Z = \text{Sn, Sb, Ge, Si}$) full Heusler alloys. Our study is based on first-principles calculations of interatomic Mn-Mn exchange interactions to set up a suitable Heisenberg spin model and on subsequent Monte Carlo simulations of the magnetic properties at finite temperature. The exchange interactions are derived from the paramagnetic state, while a realistic account of long-range chemical disorder is made in the framework of the coherent potential approximation. We find that in the case of the highly ordered alloys ($Z = \text{Sn}$ and Sb), the exchange interactions derived from the perfectly ordered $L2_1$ structure lead to Néel temperatures in excellent agreement with the experiments, whereas, in particular in the case of Si , the consideration of chemical disorder is essential to reproduce the experimental Néel temperatures. Our numerical results suggest that by improving a heat treatment of the samples to suppress the intermixing between the Mn and Si atoms, the Néel temperature of the Si-based alloys can potentially be increased by more than 30%. Based on calculated biquadratic exchange couplings, we evidence a lifting of degeneracy of the antiferromagnetic ground states on a frustrated face-centered-cubic lattice in the fully ordered compounds. Furthermore, we show that in strongly disordered Ru_2MnSi alloys, a distinct change in the antiferromagnetic ordering occurs.

DOI: [10.1103/PhysRevB.91.094432](https://doi.org/10.1103/PhysRevB.91.094432)

PACS number(s): 75.30.Et, 75.50.Ee, 71.20.-b

I. INTRODUCTION

Because of their challenging magnetic properties, Heusler alloys have attracted considerable attention in the last decades [1–3]. The possibility of tuning the magnetic and electronic properties by varying the alloy composition to a large extent, while keeping the crystal structure unchanged, provided an opportunity to verify various fundamental theoretical concepts related to magnetic alloys (see, e.g., Ref. [4] and references therein). The main reason, which brought ferromagnetic Heusler alloys to the frontline of research, is related to the possibility of full spin polarization at the Fermi level due to the half-metallic character of their electronic structures [5]. This feature is believed to have an essential impact on developing highly efficient spintronic devices [6].

Most of the magnetic Heusler alloys exhibit local magnetic moments [7] that can successfully be described in the framework of the Heisenberg spin model. It is therefore no surprise that the exchange interactions in Heusler alloys have been extensively studied on *ab initio* level [4]. Due to their possible application in magnetic shape memory devices, ferromagnetic Mn-based alloys with the chemical formula $X_2\text{MnZ}$, where X is a transition metal element and Z is a p element, gained particular interest [4,8–12]. It was widely revealed that the first nearest-neighbor (NN) magnetic interactions between the Mn atoms in the $L2_1$ full Heusler alloy crystal structure (see upper panel of Fig. 1) are strongly ferromagnetic and add the main contribution to the Curie temperature. However, if due to an excess of Mn in the alloy composition or due to chemical disorder in stoichiometric samples where Mn atoms are also present on the Z (p element) sites, they might interact antiferromagnetically with the NN Mn atoms on the proper (or original) sites, and the system might become ferrimagnetic. In particular, this is the case for the Ni_2MnAl alloy, where a

high degree of chemical disorder can be achieved by suitable thermal treatment. This material can even be a compensated antiferromagnet in the disordered B2 phase [13], which is called structurally induced antiferromagnetism [12].

The growing interest in new metallic antiferromagnets, triggered by their application in spintronic devices [14,15], focuses attention also to antiferromagnetic (AFM) Heusler alloys [16,17]. However, relatively few AFM Heusler alloys are known with sufficiently high Néel temperatures (T_N), which might raise some doubts against their application in technology. In the Ru_2MnZ ($Z = \text{Sn, Sb, Ge, Si}$) alloys the Mn moments order on the four face-centered-cubic (fcc) sublattices into the highly frustrated, so-called second kind of AFM structure (see lower panel of Fig. 1). The Néel temperatures of the Ru_2MnSi and Ru_2MnGe compounds are slightly above room temperature [18] (313 K and 316 K, respectively) and, in contrast to the relatively high temperature AFM Ni_2MnAl alloy, they are proper antiferromagnets in the fully ordered state. Ru_2MnSn has a somewhat lower ordering temperature ($T_N = 296$ K) but is still slightly above room temperature, while Ru_2MnSb has the lowest Néel temperature (195 K) in this series [18]. Recently, some attempts have been made to increase the Néel temperatures of these compounds by producing strained epitaxial films [17].

The quite low critical temperatures of the known $X_2\text{MnZ}$ AFM Heusler alloys exist for at least two main reasons. The first reason is the ferromagnetic character of the first NN Mn-Mn coupling found in first-principles calculations. In Ref. [19], the first three NN exchange couplings in the Ru_2MnZ series have been estimated from total energy calculations for a few ordered magnetic configurations. It has been concluded that the first NN interaction is ferromagnetic, and the stabilization of the AFM structure occurs due to almost equally strong

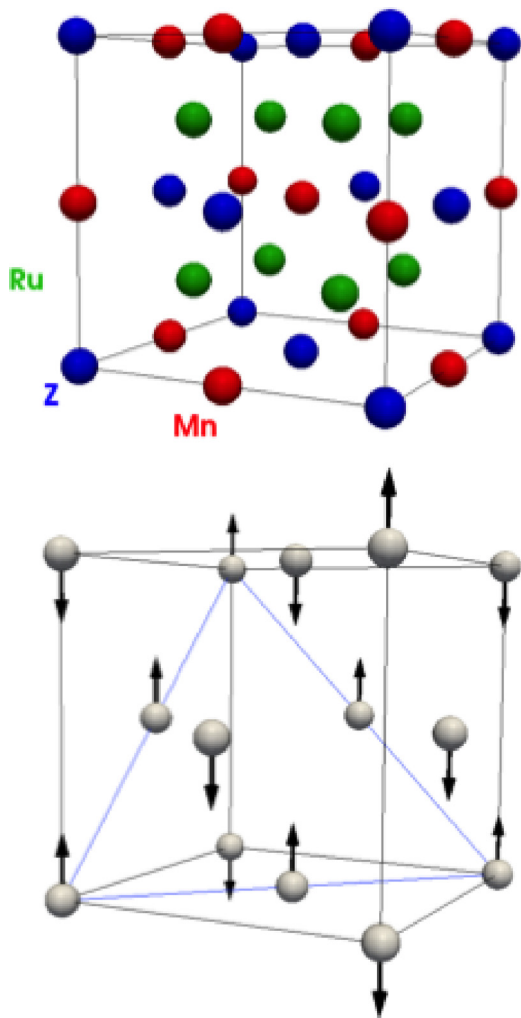


FIG. 1. (Color online) The $L2_1$ crystal structure of Ru_2MnZ alloys (upper panel) and the second kind of AFM order on the fcc sublattice of Mn atoms (lower panel).

second NN exchange coupling of AFM character. Another source of the low critical temperatures of AFM Heusler alloys is the magnetic frustration that can naturally occur on an fcc lattice. In particular, the Ru_2MnZ compounds exhibit a very special and rare type of AFM order on an fcc lattice, the so-called second kind of AFM structure [18]. As visualized in the lower panel of Fig. 1, in this type of ordering each of the four simple cubic (sc) lattices constituting the fcc lattice has a checkerboard AFM order, but the mutual intersublattice

orientation of the magnetic moments is completely frustrated. Within the Heisenberg model, this frustration can only be resolved by quantum effects, and it has been the subject of a number of theoretical investigations [20,21].

In this paper we present a first-principles study of anti-ferromagnetism in the Ru_2MnZ series of a Heusler alloy. We pay particular attention to the effects of chemical and magnetic disorder on the calculated exchange constants and on the magnetic frustration. The influence of disorder on the magnetic transition temperature in Heusler alloys was studied on a similar level of accuracy only in Ref. [22] in the case of the half-Heusler NiMnSb alloy, where the importance of the non-mean-field treatment of the chemical disorder within a Heisenberg model has been pointed out. This obviously applies to the Ru_2MnZ full Heusler alloys with nontrivial AFM ordering. The magnetic features related to the special AFM ordering will be discussed for the case of the Ru_2MnSb compound in detail. We found that in the case of $Z = \text{Si}$, the experimentally observed chemical antisite disorder on Mn and Si sublattices considerably reduces the Néel temperature, opening the way for a sample improvement in terms of a suitable heat treatment. In the case of a strongly disordered Ru_2MnSi compound, close to the disordered B2 phase, our study predicts a transition to a complex AFM structure essentially different from the second kind of AFM ordering.

II. COMPUTATIONAL DETAILS

We performed first-principles investigations within the local spin-density approximation (LSDA) [23] by using the Korringa-Kohn-Rostoker (KKR) band structure method in the atomic sphere approximation (ASA) [24,25], where the partial waves were expanded up to $l_{\text{max}} = 3$ (*spdf*-basis) inside the atomic spheres. We used the experimental lattice constants of the $L2_1$ lattice structure of the considered alloys [1] as listed in Table I. Since our main goal is to estimate the Néel temperature and the formation of the magnetic order at elevated temperatures, we determined the electronic structure self-consistently in the paramagnetic phase of the considered systems modeled within the disordered local moment (DLM) scheme in the scalar relativistic approximation [26]. Atomic disorder between the Mn and Z sublattices was treated as a random binary alloy, $\text{Ru}_2(\text{Mn}_{1-x}\text{Z}_x)(\text{Z}_{1-x}\text{Mn}_x)$ for $0 \leq x \leq 0.5$ by using the single-site coherent potential approximation (CPA) [25]. Referring to what follows, we shall denote the Mn atoms on the sites of the nominal (original) Mn sublattice by Mn(S), whereas those on the sites of the nominal Z sublattice by Mn(AS).

TABLE I. Calculated local magnetic moments of Mn atoms (m_{Mn}), first three NN exchange interactions between the Mn atoms ($J_{1\text{NN}}$, $J_{2\text{NN}}$, and $J_{3\text{NN}}$), and Néel temperatures (T_N^{calc}) for ordered Ru_2MnX compounds. The experimental lattice constant (a) and Néel temperatures (T_N^{exp}) are taken from Ref. [18]. A representative relative position vector of the corresponding Mn-Mn pair is given in units of a below the labels of the exchange interactions. The calculated first NN biquadratic coupling constants, $K_{1\text{NN}}$, are presented in the last column.

	a (Å)	$m_{\text{Mn}}(\mu_B)$	$J_{1\text{NN}}$ (mRy) [1/2 1/2 0]	$J_{2\text{NN}}$ (mRy) [1 0 0]	$J_{3\text{NN}}$ (mRy) [1 1/2 1/2]	T_N^{calc} (K)	T_N^{exp} (K)	$K_{1\text{NN}}$ (mRy)
Ru_2MnSn	6.217	3.26	0.1128	-0.4954	-0.0164	320	296	0.0033
Ru_2MnSb	6.200	3.56	0.1483	-0.2050	0.0065	180	195	-0.0055
Ru_2MnGe	5.985	3.04	0.1768	-0.4855	-0.0174	365	316	0.0010
Ru_2MnSi	5.887	2.95	0.1765	-0.5214	-0.0209	415	313	-0.0007

The magnetic properties of the Ru₂MnZ Heusler compounds can well be described by the classical Heisenberg Hamiltonian,

$$H = - \sum_{(i,j)} J_{ij} \vec{e}_i \vec{e}_j, \quad (1)$$

where the sum runs over all the different Mn-Mn pairs and \vec{e}_i denotes the unit vector pointing along the magnetic moment of the i th Mn site. In the case of chemical disorder between the Mn and Z sublattices, the sum in Eq. (1) also includes sites on the Z sublattice occupied by Mn atoms with probability x . The isotropic exchange interactions, J_{ij} , were evaluated from the DLM reference state in the spirit of the magnetic force theorem [27] as implemented within the bulk KKR method [28]. The use of the DLM reference state in the calculations of the exchange interaction constants allows for an account of the influence of the thermal magnetic disorder on the electronic structure and on the interatomic exchange interactions, thus, for a more precise estimation of the magnetic ordering temperature (see, e.g., Refs. [22,29–31]).

In order to study finite temperature magnetic properties, we performed Monte Carlo simulations with the spin Hamiltonian (1) using $16 \times 16 \times 16$ primitive cells of the underlying magnetic fcc lattice (a cluster of 4096 Mn atoms) with periodic boundary conditions. For the simulations of the chemically disordered Ru₂MnSi alloys, $12 \times 12 \times 12$ cells of both the Mn and Si fcc sublattices, i.e., a total of 3456 sites, were randomly filled with Mn atoms according to their partial occupation numbers. Note that in the Monte Carlo simulations, we considered a spin model with exchange interactions up to the 20th NN shell. Although such long-range interactions can accurately be calculated by using the magnetic force theorem [27], they cause a change of only a few Kelvins in the calculated Néel temperatures. Since their magnitudes are in the range of biquadratic interactions beyond the classical Heisenberg model (see Sec. IV), the inclusion of long-range interactions into the spin model for the purpose of Monte Carlo simulations can therefore be regarded as a rather arbitrary technical choice.

III. FULLY ORDERED $L2_1$ ALLOYS

First we performed calculations as outlined above for the Ru₂MnZ compounds in the fully ordered $L2_1$ structure. The calculated local moments of the Mn atoms, the first three NN Mn-Mn exchange interactions, and the Néel temperatures obtained from Monte Carlo simulations are summarized in Table I. The Néel temperatures are compared with the experimental values, shown in the last row of Table I. As can be inferred from Table I, the local magnetic moment of Mn in the paramagnetic state is around $3 \mu_B$ or even higher, indicating a strong localization of the moments as is usual in Mn-based Heusler alloys. Note that the variation of the values of the experimental (and calculated) Néel temperatures for the Ru₂MnZ series correlate neither with the values of the lattice constant nor with the size of the local moments of the Mn atoms. Quite obviously, the Néel temperature is determined by the Mn-Mn exchange interactions governed by the actual electronic structure depending on the type of the p element in the Z position.

In ordered Ru₂MnZ alloys, the magnetic Mn atoms fully occupy one of the four interpenetrating fcc sublattices of the $L2_1$ structure. Thus, the AFM ordering occurs on a magnetically frustrated fcc lattice. From earlier experiments [18], it is known that the magnetic structure corresponds to the second kind of AFM order that occurs due to the strong second NN AFM coupling. The first NN direct exchange is ferromagnetic, but it is clearly smaller in magnitude than the second NN AFM coupling. The competition between these two exchange couplings leads to the formation of the second kind of AFM structure on the fcc lattice.

Remarkably, the Néel temperature of the Sb-based compound is nearly two times lower than in the other compounds of the series, which can almost entirely be attributed to the decreased magnitude of the second NN interaction. Since the corresponding Mn sites are directly connected by a site occupied by the p element, one could expect that an Anderson type of superexchange mechanism is primarily responsible for this strong AFM coupling. In the case of Sb with one more valence p electron as compared to Si, Ge, and Sn, the strength of this interaction is strongly reduced. However, for metallic systems, another description of the indirect exchange mechanism, namely a Ruderman-Kittel-Kasuya-Yosida (RKKY) type of exchange via polarization of the Bloch electron states applies. Indeed, as was discussed in detail by Şaşıoğlu *et al.* [9] for Mn-based Heusler alloys, both mechanisms coexist, and there is no obvious way to determine how to unravel them within the LSDA methodology as it might be possible in correlated insulators or for less localized metals without p elements.

The Monte Carlo simulations with exchange interactions calculated up to the 20th NN shells result indeed in the second kind of AFM ordering for all the considered alloys. This is the case when taking into account only the first three NN couplings in Table I, in full agreement with the (J_1, J_2, J_3) phase diagram of the magnetic fcc lattice as given by Moran-Lopez *et al.* [32]. However, we find an essential difference between our calculated exchange interactions and earlier estimations [19] made on the basis of total energy calculations for a couple of ordered magnetic configurations. This can be understood since in Ref. [19] the authors limited their mapping procedure only to the first three NN interactions, and a similar strategy has been pursued in the theoretical analyses of the experimental data in Ref. [18]. In Fig. 2 we show the calculated values of the exchange interactions for distant pairs. Apparently, the fourth NN interactions are rather large for all compounds of the Ru₂MnZ series. Moreover, the third NN interactions are very small, even smaller than the fifth and sixth NN couplings. Thus by limiting the mapping of the total energies onto the first three NN interactions, one can make a severe numerical error in the estimated values of these exchange couplings. This nicely illustrates the advantage of the torque method [27] over the direct total energy mapping using a limited number of magnetic configurations in the case of metallic magnets with long-range exchange interactions.

One can see from Table I that the calculated Néel temperatures are in excellent agreement with the experiment for the Ru₂MnSb and Ru₂MnSn compounds but by about 50 K and 100 K higher than the experimental values for Ru₂MnGe and Ru₂MnSi, respectively. The most possible reason for this

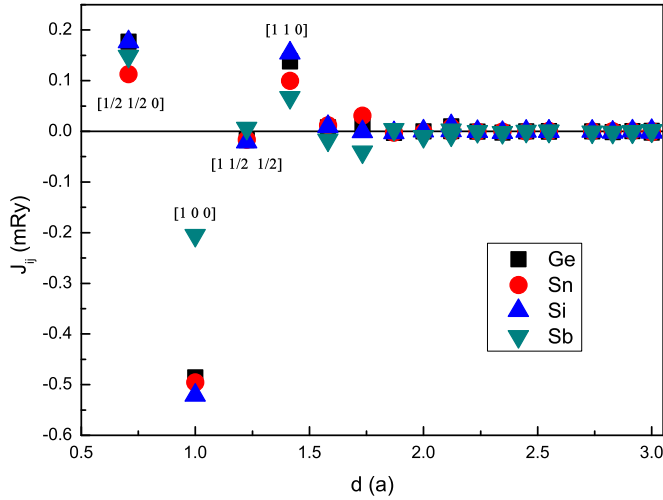


FIG. 2. (Color online) Calculated Mn-Mn exchange interactions, J_{ij} , in fully ordered Ru_2MnZ ($Z = \text{Sn}, \text{Sb}, \text{Ge}, \text{Si}$) compounds as a function of the distance, d , measured in units of the lattice constant, a . The relative position vectors of the pairs are labeled explicitly for the first four NN.

disagreement is the partial chemical disorder within the Mn and Z sublattices observed in the single crystals of Ru_2MnSi , whereas an almost perfect $L2_1$ order has been reported for Ru_2MnSb and Ru_2MnSn [18]. We will investigate the effect of partial chemical disorder on the Néel temperature after discussing the frustration effects on the magnetic correlation functions in the next section.

IV. EFFECTS OF MAGNETIC FRUSTRATION

The magnetic order in Ru_2MnZ alloys can be understood on the basis of four interpenetrating sc lattices constituting an fcc lattice, each of them possessing a checkerboard AFM order. The mutual orientations of the sublattice moments are frustrated, and this frustration is not even removed by considering more distant interactions beyond the third NN shell. In this section, we illustrate the manifestation of frustration effects in the finite temperature spin-spin correlation functions. As an example, we take the Ru_2MnSb compound, which exhibits a very high degree of chemical order [18]. The spin-spin correlation function for the n th NN shell is defined as

$$c(n) = \frac{1}{N} \sum_i \frac{1}{N_n} \sum_{\vec{R}_n} \langle \vec{e}_{\vec{R}_i} \vec{e}_{\vec{R}_i + \vec{R}_n} \rangle, \quad (2)$$

where the first sum runs over N translation vectors of the fcc lattice, \vec{R}_i ; the second sum is taken over the N_n translation vectors, \vec{R}_n , spanning the n th shell; and $\langle \rangle$ stands for the statistical average. Quite obviously, these correlation functions provide information on the magnetic short-range order in the system.

It can be easily shown that in the ordered second kind of AFM structure, the spin-spin correlation functions for the second and fourth NN shells take the values -1 and $+1$, respectively, since all the corresponding neighbors are uniformly magnetized antiparallel or parallel with respect to the atom at the arbitrarily chosen center position. In the

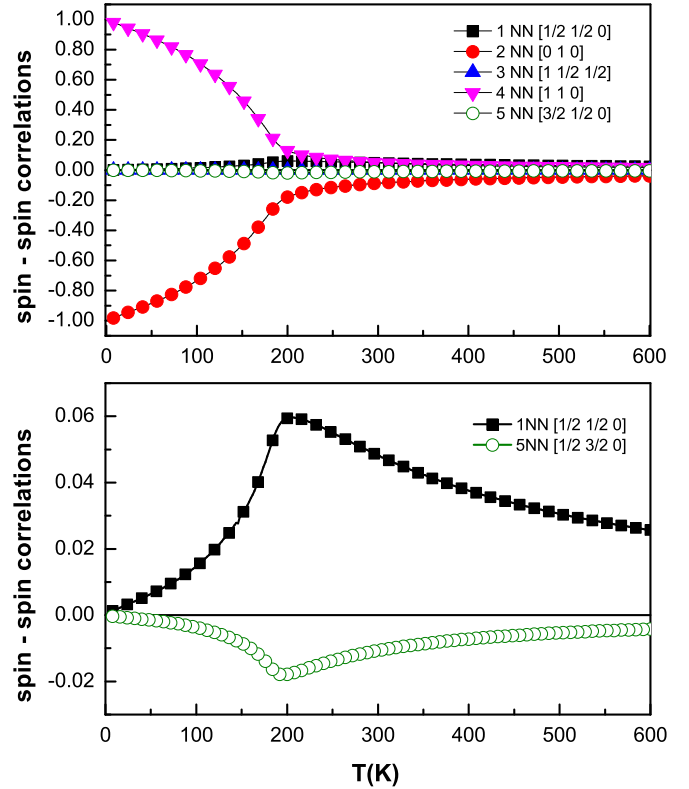


FIG. 3. (Color online) Calculated temperature dependence of the spin-spin correlation functions, Eq. (2), for the selected neighbor shells in Ru_2MnSb . Note the difference in the vertical scale of the two panels.

upper panel of Fig. 3, the temperature dependence of the spin-spin correlation functions is displayed for the ordered Ru_2MnSb alloy. At low temperatures, the functions $c(2)$ and $c(4)$ reach values close to -1 and $+1$, respectively, whereas $c(n)$, for $n = 1, 3, 5$, and 6 approach zero. The magnitudes of $c(2)$ and $c(4)$ monotonously decrease as the temperature increases. The inflection point of the curves indicates the ordering temperature, $T_N = 180$ K, in good agreement with the experimental value of 195 K.

A specific feature of the second kind of AFM structure on the fcc lattice is that the first, third, and fifth shell correlation functions (and all correlations beyond the fifth shell) vanish as the temperature approaches zero. This happens since the respective shells contain an equal number of sites with opposite magnetizations, and it is a purely geometrical consequence of the given type of ordering irrespective of the mutual orientation of the four AFM sublattices. However, since the first NN interaction in Ru_2MnSb is quite strong relative to the second and third NN interactions, a ferromagnetic short-range order likely develops in the paramagnetic phase. This is illustrated in the lower panel of Fig. 3 in terms of the temperature dependence of the spin-spin correlation functions, $c(1)$ and $c(5)$. As can be seen, these correlation functions take a finite value well above the critical temperature in the paramagnetic phase and, when the system is cooled down, they even gradually increase. Upon the onset of AFM order below the critical temperature, the respective short-range order rapidly decreases and vanishes at zero temperature. A

detailed discussion of the magnetic short-range order in the paramagnetic phase can be found in Ref. [33], where a similar analysis of the spin-spin correlation functions was performed for the AFM GdPtBi half-Heusler alloy.

The resolution of the frustration in the mutual orientation of the four AFM sublattices might happen due to small non-Heisenberg interactions and/or quantum effects. For a given type of order on the fcc lattice, Yildirim *et al.* [20] showed how the quantum effects distinguish between two possible collinear spin arrangements. However, it remained open whether these collinear states are energetically favored within the continuously degenerate manifold of noncollinear states. Recently, based on a phenomenological description, it has transparently been shown [34] that including biquadratic terms in the spin model can resolve a similar problem of magnetic orderings in ferropnictides. We therefore consider first NN biquadratic terms,

$$H_{BQ} = - \sum_{(i,j) \in \text{1NN}} K(\vec{e}_i \vec{e}_j)^2, \quad (3)$$

in an attempt to explore the stabilization of the actual magnetic ground state. For the calculations of K , we use a method described by Ruban *et al.* [35] based on the KKR formalism and the generalized perturbation methods (GPM) applied for the DLM state. The calculated values are presented in the last column of the Table I. As one can see, the biquadratic exchange interaction is nearly two orders smaller in magnitude than the leading bilinear exchange interactions, thus, they have almost no influence on the value of the Néel temperature. Note that the biquadratic interactions we calculated for the Ru_2MnZ compounds are also by one order less in magnitude than for pure body-centered-cubic (bcc) Fe calculated by the same method in the original paper on the GPM method [35]. However, the biquadratic interactions presented in Table I are still larger than the typical magnetic anisotropy energies in cubic transition metal systems and thus seem to be the leading mechanism to lift the degeneracy related to different sublattice orientations. Interestingly, the NN biquadratic interaction is positive for Ru_2MnSn and Ru_2MnGe and negative for Ru_2MnSb and Ru_2MnSi . This means that in Ru_2MnSn and Ru_2MnGe , the collinear magnetic order would be stabilized, whereas in Ru_2MnSb and Ru_2MnSi a noncollinear arrangement of the sublattice magnetizations would be favored. According to our numerical investigations, within this noncollinear arrangement the magnetization of three sublattices lie in one plane with mutual angles of 120° , and the magnetic moments in the fourth sublattice are perpendicular to this plane.

The revealed small values of the biquadratic exchange couplings leave a question open concerning the existence of additional soft gapless magnon modes associated with the rotation of the sublattice Néel vectors with respect to each other. The existence and manifestation of such modes in the highly degenerated second kind of AFM structure crucially depends on quantum effects, which partially lift the degeneracy (see discussion in Refs. [20,36]) and open a gap in the corresponding part of the magnon spectrum. Such a gap in the magnon spectrum was observed experimentally in $\text{Ca}_3\text{Fe}_2\text{Ge}_3\text{O}_{12}$ garnet [37], which possesses a similar magnetic ordering as the Ru_2MnZ compounds. Thus the

Ru_2MnZ compounds might provide an opportunity for further experimental studies of this effect, taking also into account the possibility of its control by chemical disorder in the Mn-Z sublattice.

V. EFFECTS OF CHEMICAL DISORDER ON THE MAGNETISM IN Ru_2MnSi

In order to properly describe the magnetism in Ru_2MnSi we took into account the partial chemical disorder between the Mn and Si sublattices, i.e., the presence of some fraction of Mn(AS) atoms on the Si sublattice [or, other way around, the presence of Si(AS) on the Mn sublattice]. In this section we present the results of DLM calculations for partially disordered $\text{Ru}_2(\text{Mn}_{1-x}\text{Si}_x)(\text{Si}_{1-x}\text{Mn}_x)$ alloys along the path from the $L2_1$ to the B2 phase ($0 \leq x \leq 0.5$). The calculated exchange interactions for close neighbors are shown in Fig. 4 as a function of the concentration x . Concerning the Mn-Mn pairs on the nominal Mn sublattice, the second NN AFM interaction is slightly reduced, whereas the first and fourth NN FM interactions rapidly decrease with increasing disorder and the first NN interaction even changes sign at about $x = 0.3$. It is noteworthy that the second NN Mn(S)-Mn(AS) interaction is strongly ferromagnetic, while the leading Mn(AS)-Mn(AS)

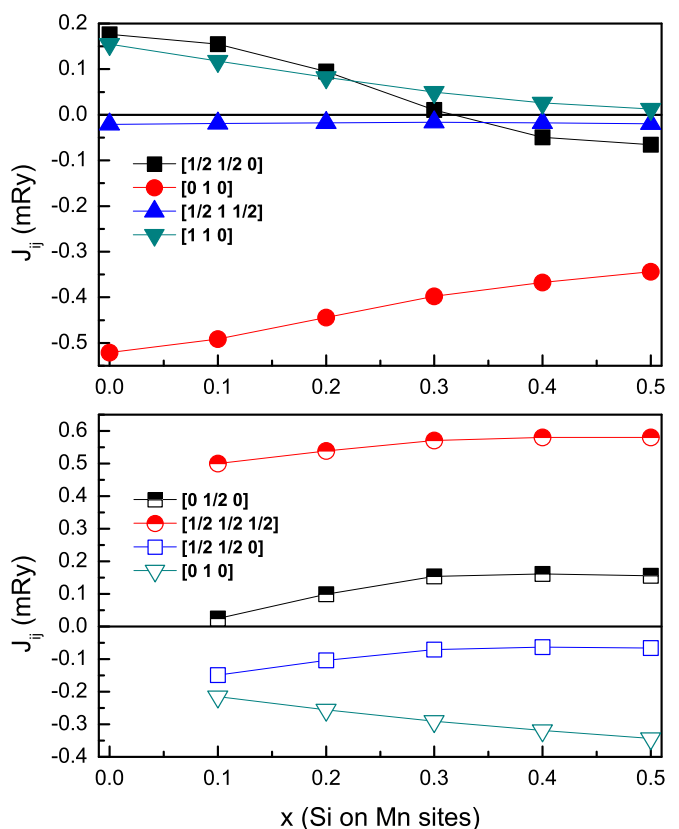


FIG. 4. (Color online) Calculated Mn-Mn exchange interactions in the partially ordered Ru_2MnSi alloy as a function of the Si concentration in the Mn sublattice. Upper panel: interactions between the Mn atoms on the nominal Mn sublattice. Lower panel: Mn(S)-Mn(AS) interactions (combined symbols) and Mn(AS)-Mn(AS) interactions (open symbols).

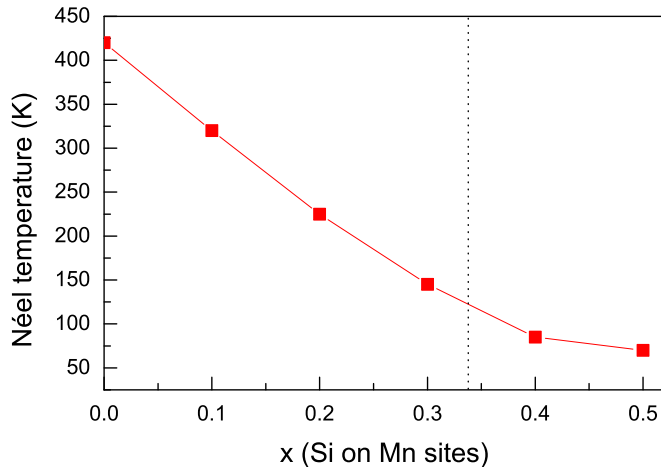


FIG. 5. (Color online) Simulated Néel temperature of the partially ordered Ru_2MnSi alloy as a function of the Si concentration in the Mn sublattice. The approximate concentration where a transition in the AFM ordering occurs (see text) is marked by a vertical line.

interactions are AFM. Clearly, the interactions for the respective Mn-Mn pairs at the proper sites and at the antisites become identical in the B2 phase ($x = 0.5$).

We performed Monte Carlo simulations where the magnetic sites were randomly distributed over the the combined Mn-Si sublattices with the prescribed concentrations. The simulated Néel temperatures are shown in Fig. 5. One can immediately see that the chemical disorder significantly decreases the Néel temperature in the Ru_2MnSi alloys. The calculated Néel temperature agrees well with the experimental one for $x(\text{Si}) = 0.1$, which is consistent with a weak disorder found in the experimental samples [18]. In addition, we can conclude that the Néel temperature of Ru_2MnSi can be increased above room temperature by producing the samples with better $L2_1$ order.

Note that in the case of partially ordered alloys, the underlying magnetic sublattice is sc. As the number of Mn atoms on the Si sublattice increases, the strong FM Mn(S)-Mn(AS) interactions start to play a dominant role, and finally the simulations predict the formations of a complex random AFM structure, being quite different from the initial second kind of AFM ordering on the fcc lattice. This AFM phase stabilizes on a strongly disordered sc lattice, and it does not correspond to any type of AFM collinear ordering on a chemically ordered sc lattice. The spin structure is periodic along the $[1\ 1\ 1]$ direction with a wave vector of $\vec{q} = [1/2\ 1/2\ 1/2]$. This periodicity is consistent with a maximum of the Fourier transform, $J(\vec{q})$, of the calculated exchange interactions for the B2 phase assuming that all sites of the underlying sc lattice are populated by Mn atoms. Our simulations thus predict the change of the type of AFM ordering on the path from the

$L2_1$ to the B2 phase. In Fig. 5, the approximate concentration where this phase transition occurs is marked by a vertical line. It is, however, not clear whether this magnetic phase can be observed in the experiment since it requires a very high degree of the chemical disorder in the Mn-Si sublattices.

VI. CONCLUSIONS

In terms of combined first-principles calculations and Monte Carlo simulations, we have shown that the AFM structure of Ru_2MnZ ($Z = \text{Sn}, \text{Sb}, \text{Ge}, \text{Si}$) full Heusler alloys is determined by a strong second NN AFM coupling between well localized Mn moments. This interaction is mediated by the p atom positioned between the interacting pair of Mn atoms. The calculations also evidence that a strong ferromagnetic fourth NN coupling strengthens the stability of a second kind of AFM structure. The calculated Néel temperatures for fully ordered $L2_1$ structures are in excellent agreement with experiment for the alloys exhibiting a very high degree of chemical ordering ($Z = \text{Sn}$ and Sb). For Ru_2MnSi , where a moderate disorder in the Mn-Si sublattice is determined experimentally, we demonstrated that the chemical disorder significantly reduces the critical temperature, and we found that the experimental Néel temperature can be reproduced with about 20% of Mn atoms on the Si sublattice. This observation might be of great importance for applications since the Néel temperature of Ru_2MnSi can be pushed well above room temperature by lowering the chemical order in the samples. Moreover, for alloys close to the B2 order, we predicted the appearance of a new AFM phase corresponding to the wave vector $\vec{q} = [1/2\ 1/2\ 1/2]$.

We also calculated biquadratic exchange interactions in order to resolve the degeneracy of the AFM ground states. We found that different signs of the biquadratic interactions across the Ru_2MnZ series lead to the stabilization of different AFM configurations in $Z = \text{Ge}, \text{Sn}$ and $Z = \text{Sb}, \text{Si}$ compounds. In the former case, the biquadratic exchange stabilizes collinear spin ordering, whereas in the latter case it leads to the formation of a complex noncollinear spin configuration. Our predictions for the magnetic ground states in the Ru_2MnZ compounds based on bilinear and biquadratic couplings from *ab initio* calculations call for experimental verification.

ACKNOWLEDGMENTS

The research leading to these results has received funding from the European Union Seventh Framework Programme (FP7/2007-2013) under Grant No. NMP3-SL-2013-604398. Financial support was also provided by the Hungarian Scientific Research Fund under Contract No. OTKA K84078.

[1] P. J. Webster and K. R. A. Ziebeck, in *Alloys and Compounds of d-Elements with Main Group Elements, Part 2*, edited by H. R. J. Wijn, Landolt-Bornstein, New Series, Group III, Vol. 19/c (Springer, Berlin, 1988).

[2] K. R. A. Ziebeck and K.-U. Neumann, in *Heusler Alloys*, edited by H. R. J. Wijn, Landolt-Bornstein, New Series, Group III, Vol. 32C, 64-314 (Springer, Berlin, 2001).

- [3] T. Graf, S. S. P. Parkin, and C. Felser, *IEEE Trans. Magnet.* **47**, 367 (2011).
- [4] I. Galanakis and P. H. Dederichs, in *Half-Metallic Alloys—Fundamentals and Applications*, Lecture Notes in Physics, Vol. 676, 311 (Springer, Berlin, Heidelberg, 2005).
- [5] I. Galanakis and Ph. Mavropoulos, *J. Phys.: Condens. Matter* **19**, 315213 (2007).
- [6] Z. Bai, L. Shen, G. Han, and Y. P. Feng, *SPIN* **02**, 1230006 (2012).
- [7] Y. Kurtulus, R. Dronskowski, G. D. Samolyuk, and V. P. Antropov, *Phys. Rev. B* **71**, 014425 (2005).
- [8] Z. Li and S. Zhang, *Phys. Rev. B* **70**, 024417 (2004).
- [9] E. Şaşıoğlu, L. M. Sandratskii, P. Bruno, and I. Galanakis, *Phys. Rev. B* **72**, 184415 (2005).
- [10] S.K. Bose, J. Kudrnovský, V. Drchal, and I. Turek, *Phys. Rev. B* **82**, 174402 (2010).
- [11] E. Şaşıoğlu and I. Galanakis, *J. Phys. D: Appl. Phys.* **44**, 235001 (2011).
- [12] I. Galanakis and E. Şaşıoğlu, *Appl. Phys. Lett.* **98**, 102514 (2011).
- [13] M. Acet, E. Duman, E. F. Wassermann, L. Mañosa, and A. Planes, *J. Appl. Phys.* **92**, 3867 (2002).
- [14] B. G. Park, J. Wunderlich, X. Marti, V. Holy, Y. Kurosaki, M. Yamada, H. Yamamoto, A. Nishide, J. Hayakawa, H. Takahashi, A. B. Shick, and T. Jungwirth, *Nat. Mater.* **10**, 347 (2011).
- [15] A. B. Shick, S. Khmelevskiy, O. N. Mryasov, J. Wunderlich, and T. Jungwirth, *Phys. Rev. B* **81**, 212409 (2010).
- [16] N. Fukatani, K. Inagaki, T. Miyawaki, K. Ueda, and H. Asano, *J. Appl. Phys.* **113**, 17C103 (2013).
- [17] N. Fukatani, H. Fujita, T. Miyawaki, K. Ueda, and H. Asano, *J. Kor. Phys. Soc.* **63**, 711 (2013).
- [18] T. Kanomata, M. Kikuchi, and H. Yamauchi, *J. Alloys Comp.* **414**, 1 (2006).
- [19] S. Ishida, S. Kashiwagi, S. Fujii, and S. Asano, *Physica B* **210**, 140 (1995).
- [20] T. Yildirim, A. B. Harris, and E. F. Shender, *Phys. Rev. B* **58**, 3144 (1998).
- [21] J.-P. Ader, *Phys. Rev. B* **65**, 014411 (2001).
- [22] B. Alling, A. V. Ruban, and I. A. Abrikosov, *Phys. Rev. B* **79**, 134417 (2009).
- [23] J. P. Perdew and Y. Wang, *Phys. Rev. B* **45**, 13244 (1992).
- [24] I. A. Abrikosov and H. L. Skriver, *Phys. Rev. B* **47**, 16532 (1993).
- [25] A. V. Ruban and H. L. Skriver, *Comp. Mater. Sci.* **15**, 119 (1999).
- [26] B. L. Gyorffy, A. J. Pindor, J. Staunton, G. M. Stocks, and H. Winter, *J. Phys. F: Met. Phys.* **15**, 1337 (1985).
- [27] A. I. Liechtenstein, M. I. Katsnelson, V. P. Antropov, and V. A. Gubanov, *J. Magn. Magn. Mater.* **67**, 65 (1987).
- [28] A. V. Ruban, S. I. Simak, S. Shallcross, and H. L. Skriver, *Phys. Rev. B* **67**, 214302 (2003).
- [29] S. Khmelevskiy and P. Mohn, *J. Phys.: Condens. Matter* **24**, 016001 (2012).
- [30] S. Khmelevskiy and P. Mohn, *Appl. Phys. Lett.* **93**, 162503 (2008).
- [31] A. Deák, E. Simon, L. Balogh, L. Szunyogh, M. dos Santos Dias, and J. B. Staunton, *Phys. Rev. B* **89**, 224401 (2014).
- [32] J. L. Moran-Lopez, R. Rodriguez-Alba, and F. Aguilera-Granja, *J. Magn. Magn. Mater.* **131**, 417 (1994).
- [33] S. Khmelevskiy, *Phys. Rev. B* **86**, 104429 (2012).
- [34] A. L. Wysocki, K. D. Belashenko, and V. P. Antropov, *Nat. Phys.* **7**, 485 (2011).
- [35] A. V. Ruban, S. Shallcross, S. I. Simak, and H. L. Skriver, *Phys. Rev. B* **70**, 125115 (2004).
- [36] A. N. Ignatenko, A. A. Katanin, and V. Yu. Irkhin, *JETP Lett.* **87**, 555 (2008).
- [37] Th. Bruckel, B. Dorner, A. Gukasov, and V. Plakhty, *Phys. Lett. A* **162**, 357 (1992).